Journal of Solid Mechanics Vol. 15, No. 4 (2023) pp. 352-368
DOI: 10.60664/jsm.2024.3081788

Research Paper

Nonlinear Hybrid Bistable Vibration-Energy-Harvester Modeling Considering Magnetostrictive and Piezoelectric Behaviors

K. Niazi, M.J. Kazemzadeh-Parsi [*] , M. Mohammadi

Department of Mechanical Engineering, Shiraz Branch, Islamic Azad University, Shiraz, Iran

Received 27 August 2023; accepted 20 September 2023

ABSTRACT

The present study investigates a novel two degrees of freedom (2DOF) modeling of hybrid-bistable vibration energy harvester (VEH) considering nonlinear magnetic interaction and elastic magnifier to improve the efficiency and expand the action bandwidth. The main part of harvesting mechanism is a composite cantilever beam consists of three layers of magnetostrictive, piezoelectric and a metallic core with internal damping. Such a novel architecture generates more electrical power and operates at larger bandwidth than common piezoelectric or magnetostrictive energy harvesting systems. In the present work, a coupled 2DOF model is developed to investigate the vibration behavior and energy harvesting rate of the harvester. The harmonic balance method is used to obtain the frequency responses and then the Runge-Kutta method is utilized to calculate the dynamic responses. A parametric study is done to investigate the effects of the key features of the harvester such as magnets distances, base acceleration level and excitation frequency on the rate of electricity generation.

Keywords: Energy harvesting; Lumped parameter Time and frequency responses; Runge-Kutta method; Harmonic balance method.

1 INTRODUCTION

VIBRATION Energy Harvester (VEH) systems are becoming popular due to need for low rated power sources for electronic devices and also accessibility of the vibrating sources [1]. With rapidly progress of VEHs, many researchers have been considered piezoelectric energy harvesters (PEHs), magnetostrictive energy harvesters (MEHs) [2], electromagnetic and electrostatic based VEH systems to be able to extract energy from broadband

[*]Corresponding author. Tel.: +989171031282.
E-mail address: mjparsi@gmail.com (M.J. Kazemzadeh-parsi)

frequency extensively. Through the recent years, the nonlinear bistable energy harvesting (BEH) systems has received extensive attentions, since act over a further wide range of base excitation frequencies and can lead to extra output power [3]. The BEH can produce a large amplitude motion with high power by means of broadening the bandwidth greatly. Nonlinear magnetic repulsion load is one of the most conversant arrangements for BEH where can significantly growth the generated voltage and power [4].

Ferrari et al. [5] obtained the displacement response of a BPEH (Bistable PEH) under band-limited excitation and confirmed the model with experimental results. Utilizing perturbation method, Karami and Inman [6] investigated the initial resonance response of BPEH. Kim and Seok [7] considered dynamic response of multi stable VEH to harvest voltage in a wideband frequencies, even at low excitation amplitudes. Jiang et al. [8] proposed a lumped parameter model with magnetic interaction for enlargement the range of resonance frequency of bistable VEH. Nguyen et al. [9] established the magnetic interaction for 2-DOF bistable VEH producing high-energy oscillation and improved the generating power. Also Wang et al. [10] used nonlinear magnetic force to creating the electro-magnetic BEH for improving the efficiency and broadening the harvester resonance bandwidth. Optimization of harvested power of both rectangular and trapezoidal bimorph piezoelectric cantilever beams with tip mass have been investigated by Kianpour and Jahani [11] analytically. Dynamic behavior of functionally graded carbon nanotube reinforced piezoelectric cantilever harvesters have been considered by Heshmati and Amini [12] by means of finite element method.

In addition to the bistable vibration energy harvesting systems, the tri-stable vibration energy harvesting systems has attracted the attention of researchers. The reason for using tri-stable oscillators compared to linear and bistable systams is that tri-stable oscillators perform better in terms of broadband resonance frequency and lower excitation threshold. Rezaei et al. used the tri-stable non-linear restoring force in order to increase the energy harvesting and efficiency of the piezoelectric harvester. [13, 14] They also investigated the simultaneous effects of two hard excitations for the piezoelectric energy harvester. The results showed that when superharmonic and combinations resonances exist simultaneously in the system response, the generated voltage and power increase. [15]

Elastic magnifiers are mostly modeled using a linear mass-spring system. Using finite element theory, Aladwani et al [16] analyzed a PEH with elastic magnifier. A double beam VEH with elastic magnifier reported by Vasic et al. [17] to obtain the harvesting power and vibrational behavior. Utilizing lumped parameter formulation, dynamic analysis of BPEH with Elastic Magnifier have been reported by Wang and Liao [18] with the aid of harmonic balance method. Large-amplitude oscillation of cantilever BPEH has been reported by Wang et al.[19] using an auxiliary mass-spring magnifier to overcome the potential wells. Bernard and Mann [20] coupled the structures of VEH and dynamic amplifier to increase the harvesting bandwidth and harvested voltage.

Because of high energy density, Vibration based Magnetostrictive energy harvester (MEH) have gradually developed in recent years. Nowadays the researchers has been attracted to MEH, since the MEH does not require high equivalent impedance and avoids the leakage problems and depolarization, in comparison with the PEH [21]. Ueno et al. [22] established a bimorph energy harvester based on two cantilever beams made of MsM. Kita et al. [23] analysed MEH made of Fe-Ga alloy (Galfenol) with 35% of conversion efficiency. Energy harvesting and Damping of the vibration based MEH has been analysed by Fang et al. [24]. Dynamic response of a magnetostrictive VEH has been investigated by Ahmed et al.[25], using the finite element model. Cao et al. [26] considered the nonlinear vibration analysis of MEH consist of a cantilever beam with elastic magnifier, analytically and examined the effects of magnifier on the harvested power. By means of harmonic balance method and COMSOL Multiphysics software, Zhang et al.[27] studied vibration control and energy harvesting of NES-magnetostrictive coupled model made by cantilever beam. Liu et al. [28] investigated the nonlinear vibration analysis of bistable vibration MEH with dynamic magnifier. In their study, the bistable motion was formed by nonlinear magnetic force between repulsive magnets. Goudarzi et al. [29] considered a hybrid piezoelectric-pyroelectric harvesting systems made by cantilever beam with PZT and lead magnesium niobate–lead titanate, were subjected to vibration and sinusoidal heat loads. A 2DOF hybrid piezoelectric-electromagnetic energy harvester has been considered by Wang et al.[30] to enhance the collected power from the electromechanic transducer. Sengha et al. [31] investigated stochastic dynamic analysis of the hybrid energy harvester with the nonlinear magnetic coupling. Jahanshahi et al. [32] studied dynamic behavior of hybrid piezo-magnetoelastic based harvester under low frequency excitations and multi-frequency excitations. Bistable rotational energy harvesting systems with hybrid piezoelectric - electromagnetic mechanisms have been reported by Fang et. al.[33] for growing output voltage at the low-frequency excitation. Lia et al. [34] considered mathematical Modeling of vortex shedding-induced vibration behavior of piezoelectric-electromagnetic hybrid energy harvesters. Magneto-rheological fluids are also another type of advanced materials which are considered in vibration analysis of smart materials and interested readers can refer to [35, 36].

In our previous work, [37], we employed an analytical procedure to consider dynamic analysis of a novel 2DOF hybrid VEH based on both piezoelectric and magnetostrictive mechanisms considering a dynamic magnifier using lumped parameter model. The influence of magnifier parameters have been examined on the time and frequency response features, in detail. In the present study, a hybrid 2DOF VEH consists of a three-layered architecture of a cantilever beam with core and smart layers (piezoelectric and magnetostrictive) is considered while taking into account the nonlinear interaction of the magnets. Based on our best knowledge, the effect of metallic core damping and the distance between two magnets on the electromechanic behavior, have been considered here for the first time. A parametric study is done to provide a theoretical background to be used for practical design of hybrid MS-P VEH.

2 NOVEL HYBRID VIBRATION ENERGY HARVESTER

A schematic representation of the main components of the Hybrid Magnetostrictive Piezoelectric (HMP) vibration harvesting system with elastic magnifier (EM) is shown in Fig.1. The hybrid power generation system consists of a composite cantilever beam made of three layers of base matalic core and magnetostrictive and piezoelectric layers at top and bottom of the core. The thickness of the piezoelectric, magnetostrictive and the metalic base are shon respectively by h_p , h_m and h_b. The total efective legnth of the beam is l which consists of two parts, $l = l_b + l_v$ (as seen at Fig.1).

In the present study, the whole vibrating system is simplified to a 2-DOF lumped parameter vibration model, in which M_0 and K_0 denote the equivalent mass and stiffness of the elastic magnifier, respectively. The equivalent mass, stiffness and damping of the cantilever beam are M_e , K_e, and C_e respectively. Where [38]:

$$M_e = M_t + \frac{33}{140}m;(M_t = \rho_A \times V_A);K_e = \frac{3EI_b}{L^3} \tag{1}$$

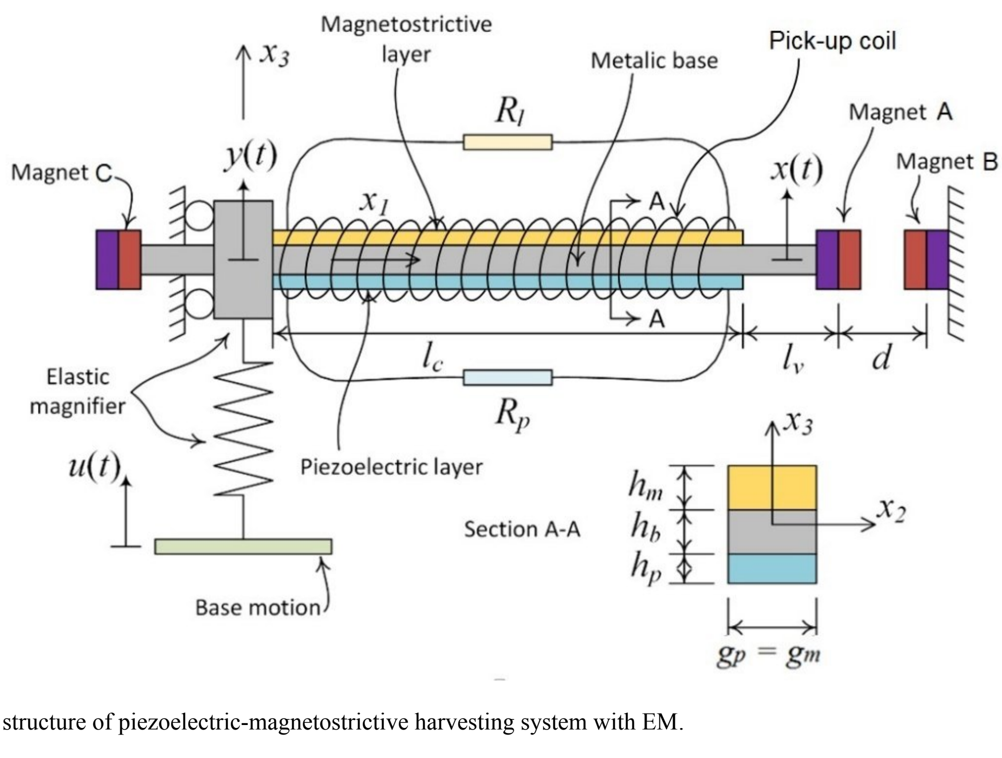

Fig.1
Schematic structure of piezoelectric-magnetostrictive harvesting system with EM.

In which M_t is the tip mass and equals to the product of the density and the volume of the tip magnet. Also *m, E* and ζ are the composite beam's mass, Young's modulus, and damping ratio, respectively. I_b is the moment of inertia of the beam cross section about the neutral axis and EI_b is the average stiffness of the beam. the mass ratio r_m and stiffness ratio r_k of the harvester are introduced as:

$$r_m = M_0/M_e\,;\; r_k = K_0/K_e \tag{2}$$

The surface of piezoelectric layer are completely enclosed with tinny electrode and an resistance R_P is coupled to the piezoelectric energy harvester electrically. Also A pick-up coil , with resistance R_c , turns N, length $l_c \approx l_m$, and cross-sectional area $S_c \approx g_m h_m$, in which g_m is beam width ,is bounded on the cantilever and linked in series with resistance R_L the power collection part is simplified as the load impedance.

Two magnets A and C, provide a bias magnetic field $H_b = 3580\ A/m$ for the Ms layer. Magnets A, B, and C have the same volume , $V_A = V_B = V_C$, and their magnetization are M_A, M_C and M_B. The beam's longitudinal axis is x_1, whereas the transverse axis is x_3, so that the x_1 - x_3 plane is set on the neutral plane of the beam. The EM consisting of a mass, and a spring element and positioned between the BHEH and the base. An acceleration $\ddot{u}$ is applied to the base and the displacement of the mass M_e and M_0 are written as $x_e(t)$ and $y(t)$, respectively.

As shown in Fig.1 magnet A is attached to the beam free end; its magnetic field direction is reverse polarity to the field of another fixed magnet B. The two-part permanent magnets are mutually repellentand creates a bistable structure. The magnet interaction is the nonlinear vertical force F_N , Based on the taylor series is [28]:

$$F_N = k_1(x_e - y) + k_3(x_e - y)^3$$

$$k_1 = \frac{\frac{3}{2}\mu_0 V_A V_B M_A M_B}{\pi d^4};\, k_3 = k_1(1/l^2 + 5/d^2) \tag{3}$$

The distance between two magnets A, B are denoted by d ,measured acording to the undeformed shape of the beam. By adjusting the parameter d , the force between them is varied. When this distance is proper, the system is bistable. The system currently has two steady-state equilibria, and the harvester displays bistable features.

3 MATHEMATICAL MODELING OF HARVESTING SYSTEM

3.1 Magnetostrictive Layer

When the harvester vibrates, because of the villari effect the magnetic induction B_z in Ms material (Galfenol) is varied, so the current i and magnetic field H_z in the coil are induced, In which:

$$H_c = Ni/l_c \tag{4}$$

In which N is the Number of coil turns. The constitutive equations for Ms layer are [36]:

$$\varepsilon_M = \frac{\sigma_M}{E_M + d_M H_z}$$

$$B_z = d_M \sigma_M + \mu H_z \tag{5}$$

Where ε_M denotes the strain, $H_z = H_b + H_c$ signifies the strength of magnetic field , σ_M is the stress applied to the Ms, E_m is the Young's modulus of the Ms; d_M is piezomagnetic coefficient and μ is magnetic permeability. The average stress $\sigma^i{}_M$ associated with i is given as [39]:

$$\sigma_M = d_M k_M (2l - l_m)\tilde{h} i / 4I_b$$
$$k_M = \frac{4E_M I_b N_c}{\tilde{h}(2l - l_m) l_c} \tag{6}$$

where, $\tilde{h}$ is the distance from the neutral axis of beam cross section to the center of Ms layer. x is the relative displacement of the beam tip and l is the beam effective length as mentiond before.

From Eqs. (5),(6) the magnetic field strength B_z can be found as :

$$B_z = d_M E_M \tilde{h} x / l^2 + (\mu - E_M d_M{}^2)(H_b + N_c i / l_c) \tag{7}$$

As mententiond before, H_b is the biased magnetic field providing for the magnetostrictive material. Considering the electrical part of the Ms layer, the induced current i in the pick-up coil with length l_c using faraday law, is [40]:

$$R_M \frac{di}{dx_1} = \frac{-N_c S_c}{l_c} \frac{dB_z}{dt} \tag{8}$$

Where R_M =(R_L+R_C), in which R_C , R_L are the coil resistance and load resistance, respectively. Replacing Eq. (7) into Eq. (8) and participating the subsequent equation with respect to x_1 yields the harvested voltage of the Ms harvester part as:

$$V_M = \beta \frac{dx}{dt} - L_M \frac{di}{dt} \tag{9}$$

In which [39] :

$$\beta = \frac{1}{6} N_c S_c E_M d_M \tilde{h}(2l - l_m) / l^3$$
$$L_M = (\mu - E_M d_M{}^2)(N_c{}^2 S_c / l_c) \tag{10}$$

So the electrical equation of the Ms is expressed as:

$$\beta \frac{dx}{dt} - L_M \frac{di}{dt} - R_M i = 0 \tag{11}$$

3.2 Piezoelectric layer

For the piezoelectric layer attached on the cantilever beam, the piezoelectric constitutive equation can be written as [38, 41, 42]:

$$\varepsilon_p = s_{11}\sigma_p + d_{31}E_z$$
$$D_z = d_{31}\sigma_p + \varepsilon_{33}^T E_z \tag{12}$$

Where E_z and D_z characterize the electric field and displacement in the z-direction, consistently. ε_p is the strain in the x_1-direction; s_{11} is the compliance coefficient under a constant electric field; σ_p is the stress in the x_1-

direction; d_{31} is the piezoelectric coefficient; E_z is the electric field strength in the x_3-direction; D_z is the electric displacement in the x_3-direction; $\varepsilon^T{}_{33}$ is Dielectric coefficient under constant stress. The average stress σ_p associated with v is given as follow [43]:

$$\sigma_p = -\frac{1}{4}k_v v(2l - l_e)(h_p + h_b)/I$$
$$k_v = \frac{4Ie_{31}}{h_p(2l - l_e)(h_p + h_b)} \tag{13}$$

h_b is the thickness of the cantilever beam, l_e is the length of the piezoelectric layer. Also e_{31} is the piezoelectric constant. Consider the relationship between the displacement x and the generated, It can be obtained from Eq. (13):

$$D_z = d_{31}\sigma_p = \frac{3}{4}e_{31}(2l - l_e)(h_p + h_b)x/l^3 \tag{14}$$

where E_p is the elastic modulus of the piezoelectric layer, Then:

$$\frac{dv}{R_p dt} = 2bl_e\frac{dD_z}{dt} = k_p\frac{dx}{dt}$$
$$k_p = \frac{3bl_e e_{31}(2l - l_e)(h_p + h_b)}{2l^3} \tag{15}$$

Considering the Piezoelectric part, the electrical equation based on the Kirchhoff's law is expressed as [36]:

$$k_p\frac{dx}{dt} + \frac{v}{R_p} + C_p\frac{dv}{dt} = 0 \tag{16}$$

Where v, C_p and R_p are the voltage, capacitance and resistance of the piezo part, respectively.

4 COUPLING MODEL AND EQUATION OF FORMATION

The coupled nonlinear equations of the hybrid 2-DOF harvester may be found by combination of the ordinary differential equations of the Ms and piezoelectric parts as follows, Using relative motion x, $(x = x_e - y)$.

$$M_e\frac{d^2y}{dt^2} + M_e\frac{d^2x}{dt^2} + C_e\frac{dx}{dt} + (K_e - k_1)x + k_3x^3 - k_v v + k_M d_M i = 0 \tag{17a}$$

$$M_o\frac{d^2y}{dt^2} + K_o y - (K_e x + C_e\frac{dx}{dt}) + k_v v - k_M d_M i - K_o u = 0 \tag{17b}$$

$$k_p\frac{dx}{dt} + \frac{v}{R_p} + C_p\frac{dv}{dt} = 0 \tag{17c}$$

$$\beta\frac{dx}{dt} - L_M\frac{di}{dt} - R_M i = 0 \tag{17d}$$

This study uses Runge-Kutta method to solve coupled Eqs. (17a)-(17d) and investigate the temporal output behaviours of the harvester.

5 FREQUENCY RESPONSE OF THE SYSTEM

Firstly, utilizing the four coupled equations, by omitting *y(t)*, a 4th-order nonlinear differential equation is attained as:

$$\frac{r_m}{r_k}x^{(4)}+2\zeta\eta x^{(3)}+(\frac{r_k-ar_m+1}{r_k})x''+2\zeta x'-ax+\frac{k_3}{K_e}x^3+\frac{k_3}{K_e}(6xx'^2+3x^2x'')$$
$$+\frac{(k_i d_M)^2}{K_e M_e g}i+\eta\frac{k_i d_M}{K_e}i''-\frac{g}{\omega_e^2}v-\eta\frac{g}{\omega_e^2}v''+u''=0 \tag{18}$$

In which: $\omega_e=\sqrt{\frac{K_e}{M_e}};\zeta=\frac{C_e}{2\sqrt{K_e M_e}};\eta=\frac{r_m+1}{r_k};a=\frac{k_1}{K_e}-1$

The harmonic base excitation is equals to $u''=-A_{ex}\sin\Omega t$, where Ω, A_{ex} are the excitation frequency and acceleration amplitude, respectively.

The frequency domain solution of the nonlinear hybrid harvester studied by HBM. The convergence of this method is conquered by the selected harmonics. Based on HBM, the periodic displacement, voltage and current response can be written in the form of a Fourier series expansion, as:

$$\begin{Bmatrix} x \\ v \\ i \end{Bmatrix}=\sum_{k=1}^{n}\left[\begin{Bmatrix} a_{1,k} \\ b_{1,k} \\ c_{1,k} \end{Bmatrix}\cos(k\Omega t)+\begin{Bmatrix} a_{2,k} \\ b_{2,k} \\ c_{2,k} \end{Bmatrix}\sin\Omega t(k\Omega t)\right] \tag{19}$$

In which, n is the highest harmonic order and k is the modal order. Substitution of Eq. (19) into Eqs. (17a)- (17d) gives coupled functions of harmonic coefficients. The steady-state response of the harvester can be obtained after the harmonic coefficients are solved out.

Without losing the generality, only first harmonic has been considered for the following calculations since the nonlinearity in the coupled equations of system is weak and the lumped parametes with linear strains considered [44]. Based on HBM, first order periodic solution of the vibration, voltage and current are respectively defined by:

$$\begin{Bmatrix} x \\ v \\ i \end{Bmatrix}=\begin{Bmatrix} a_{1,1} \\ b_{1,1} \\ c_{1,1} \end{Bmatrix}\cos\Omega t+\begin{Bmatrix} a_{2,1} \\ b_{2,1} \\ c_{2,1} \end{Bmatrix}\sin\Omega t \tag{20}$$

Substituting Eqs. (20) into Eqs. (17a)-(17d), equaling the coefficients of $\sin\Omega t$ and $\cos\Omega t$, respectively, six equations around variable coefficients $a_{1,1}$, $a_{2,1}$, $b_{1,1}$, $b_{2,1}$, $c_{1,1}$, $c_{2,1}$ can be obtained. After some mathematical operation this relations for frequency response are reported:

$$D_2 a_{2,1}+D_1 a_{1,1}+D_3 b_{2,1}+D_4 c_{2,1}=-A_{ex} \tag{21a}$$

$$D_2 a_{1,1}-D_1 a_{2,1}+D_3 b_{1,1}+D_4 c_{1,1}=0 \tag{21b}$$

Where:

$$D_1=\zeta(-2r_k\Omega+2\Omega^3+2r_m\Omega^3)/r_k$$
$$D_2=\frac{3k_3}{4K_e}A^2+(-\Omega^2-r_k\Omega^2+r_m\Omega^4-a(r_k-r_m\Omega^2)+\frac{3k_3}{2K_e}r_m\Omega^2A^2)/r_k$$
$$D_3=\frac{g(-r_k+\Omega^2+r_m\Omega^2)}{r_k\omega_e^2} \tag{22}$$
$$D_4=\frac{k_M d_M(r_k-(1+r_m)\Omega^2)}{r_k K_e}$$

Also $A^2=a_{1,1}^2+a_{2,1}^2$, represents the vibration amplitude of the beam tip. Utilizing Eqs. (21a) and (15b), frequency response relation can be derived as:

$$(D_2-D_3\frac{\kappa^2\Omega^2}{\theta_1^2+\Omega^2}+D_4\frac{\theta_2\Omega^2}{\alpha^2+\Omega^2})^2+(D_1+D_3\frac{\theta_1\kappa^2\Omega}{\theta_1^2+\Omega^2}-D_4\frac{\alpha\theta_2\Omega}{\alpha^2+\Omega^2})^2A^2=A_{ex}^2 \tag{23}$$

$$\kappa^2 = \frac{k_v k_p}{C_p M_e g}; \alpha = \frac{R_M}{\omega_e L_M}; \theta_1 = \frac{1}{\omega_e L_M}; \theta_2 = \beta \frac{k_M d_M}{M_e g L_M} \tag{24}$$

Obtaining $v^2 = b_{1,1}{}^2 + b_{2,1}{}^2$, $i^2 = c_{1,1}{}^2 + c_{2,1}{}^2$,the harvested power of each circuit can be obtained. Then the total output power is sum of them and equals to:

$$P_T = \frac{v^2}{2R_p} + \frac{R_M}{2} i^2 \tag{25}$$

6 NUMERICAL RESULTS AND DISCUSSION

6.1 Validation

To confirm the accuracy of the 2DOF PMEH mathematical model, this study used a PEH for justification. Geometric properties of the Bistable harvester + EM are: $L = 62mm, b = 18mm, (h_c, h_p) = (0.16, 0.2)mm$, $M_t = 5.5gr, d = 24mm$ and r_m=r_k=5; and other electromechanical data are in Table 1. The comparison of results with Ref. [18] have been shown in Table 1 for both forward and backware frequency sweep responses; the deflection results showed good agreement.

Also to confirm the accuracy of the novel PMEH mathematical model, this study used a MEH without EM, at A_{ex} *=2g* for validation. Frequency Response diagram has been plotted at Fig. (2a) at two different magnet distance. The results showed good agreement with Cao et al. [26].

Moreover, Phase portrait of MEH + EM compared with Ref. [28], when excitation level is A_{ex}=*3g* are plotted in Fig. (2b). It can be found both results are similar and the beam tip vibrate between the two steady-state positions and exhibit bistable characteristics.

Table 1
Validation of frequency response curves with Ref [18]

Excitation Frequency (Ω/ω_e)	Forward frequency sweep response		Backward frequency sweep response	
	Ref [15]	Present	Ref [15]	Present
0.2	0.56	0.58	0.24	0.25
0.4	0.71	0.74	0.14	0.16
0.6	0.93	0.97	0.11	0.13
0.8	1.26	1.32	0.12	0.14
1	0.55	0.60	0.55	0.59
1.2	0.07	0.08	0.07	0.08

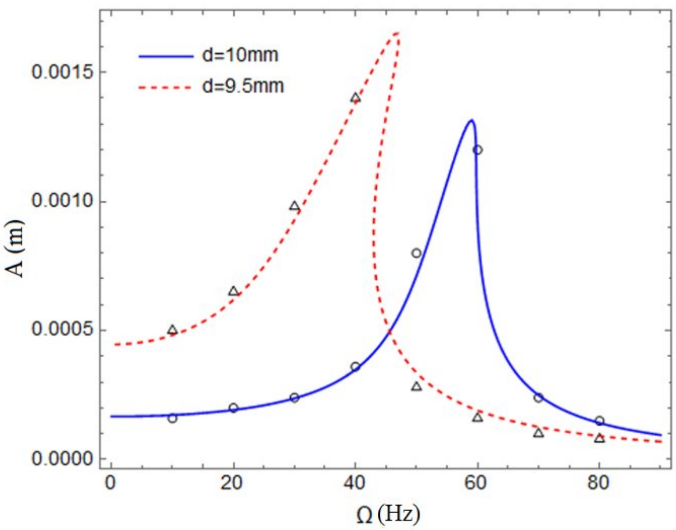

Fig.2a
Validation of FR curve with Cao et al. [26] (the present results shown by lines and markers are reference result, circle:d = 10 mm,triangle:d = 9.5 mm).

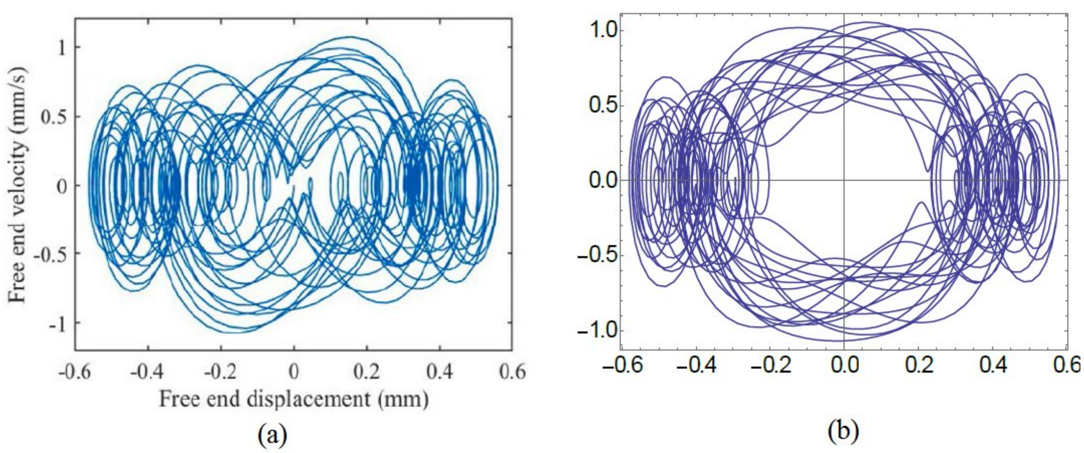

Fig.2b
Comparison of Dynamic response; (a) Ref. [28] (Taylor's method), (b) Present study (Runge-Kutta method); The difference between results comes from the method of solution.

6.2 Prametric Analysis

The Geometrical, Physical and electromechanical properties of model are listed in Table 2.

In the Fig.3a, two response peaks are noticed for each curve in which occurred at the natural frequencies of the 2DOF nonlinear system. The smaller natural frequency is related to the elastic amplifier, in which its value is independent of parameter *"d"* at $\Omega = 165\ Hz$. The response amplitude of the beam tip are equals to $A=1.49\ mm$, $A=1.21\ mm$ and $A=0.61\ mm$ in the case of increasing the excitation frequency (Forward frequency sweep response) when $\Omega = 165\ Hz$, for the case $d=7\ mm$, $d=6\ mm$ and $d=5\ mm$, respectively. Another important fact was, as parameter *"d"* decreases, the linear stiffness of the harvester increases but its nonlinear stiffness decreases. This issue can be seen in the change of the second natural frequency of the equivalent 2DOF system. Increasing of the stiffness has led to rise in the natural frequency,so by reducing *"d"* from *7mm* to *6mm* and then to *5mm*, the response peak occures at the frequency of $\Omega = 196\ Hz$, $\Omega = 234\ Hz$ and $\Omega = 365\ Hz$, respectively. Also, the amplitude of the response peaks were also strongly influenced by this parameter and have decreasing trends. The 2nd peak responses have been decreased from *A=0.75 mm* (for *d=7mm*) to *A=0.07 mm* (for *d=5mm*).

In Fig. 3b, the Frequency-amplitude curves of beam tip are plotted to investigate the effects of EM on the dynamic responses. there are two resonance peaks in all curves except in the harvester without EM. Also at second peak response curves bend to the right obviously, because of the nonlinear magnetic interaction. With no EM, the resonant frequency is **Ω** = *136 Hz* and the peak amplitude is *A=0.49 mm*, also there are one unstable solution in the frequency range $128Hz < \Omega < 136Hz$, for this curve. As showed in fig. 3b, for $r_m = r_k = 10$, resonant frequencies are **Ω** = *170 Hz* and **Ω**=*200 Hz*; and the peak amplitudes are *A=1.93mm*, *A=0.75mm*, correspondingly. When excitation frequency was in these two regions: $142Hz < \Omega < 170Hz$ or $194Hz < \Omega < 200Hz$, there are three solutions for the frequency response (two stable solution and one unstable solution). Also there are four jump points in response curve (M→N, M'→N' for Forward frequency sweep response, P→Q, P'→Q' for (Backward frequency sweep response)). On the other hand, by increasing the frequency from *0* to **Ω** = *250 Hz*, at two bifurcation points M and M', jump phenomena occurred and cause to jump down the response from upper stable branch to lower stable branch. Likewise by reducing the frequency from **Ω** = *250 Hz* to 0, the response jump up at two bifurcation points P'and P. Furthermore, when $r_m = r_k = 20$, there are just two bifutcation points at **Ω** = *192 Hz* and **Ω** =*202 Hz*; the unstable region limited to $192Hz < \Omega < 202Hz$ and the stability of system increased.

Table 2
Physical and material propertirs of the model , including piezoelectric and MsM.

Parameters	Values
Layer thickness (mm)	$h_p = 0.5; h_m = 0.75; h_b = 1.25$
Beam width (mm)	$g_p = g_m = g_b = 8$
Beam Lengths (mm)	$l_p = 32; l_m = l_b = 38; l_v = 20$
Elastic modulus (GPa)	$E_p = 66; E_m = 70; E_b = 68$
Density (g/cm^3)	$\rho_m = 2.7; \rho_b = \rho_p = 7.8; \rho_A = 8$
Magnet volume (mm^3)	$V_A = 5.13 \times 14.14^2, V_B = V_A$
Magnet intensity ($10^6 A/m$)	$M_A = 3.2, M_B = 1, M_C = 1.8$
Magnetic permeability (*H/m*)	$\mu = 230\mu_0; \mu_0 = 4\pi \times 10^{-7}$
Load resistance (*ohm*)	$R_c = 36; R_M = 100; R_p = 25000$
Dielectric permittivity (*F/m*)	$\varepsilon_{33} = 1800\varepsilon_0; \varepsilon_0 = 8.85 \times 10^{-12}$
Piezoelectric constant($10^{-12} C/m$)	$d_{31} = 190$
Piezomagnetic coefficient ($10^{-9} T/Pa$)	$d_M = 34$

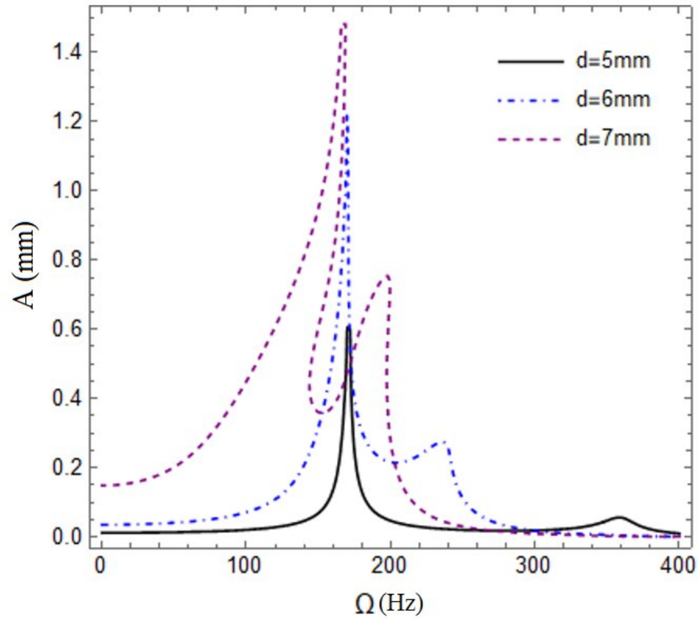

Fig.3a
Frequency response of beam tip at different magnet apace "d", when $r_m = r_k = 10$, $A_{ex} = 2g$.

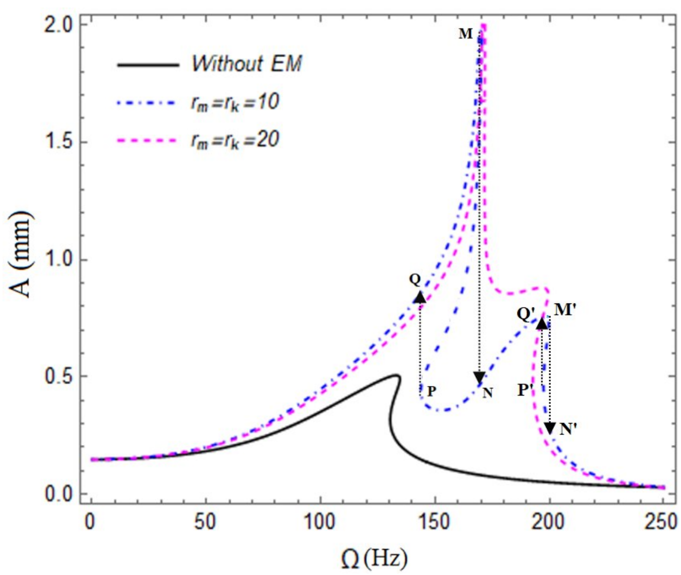

Fig.3b
Frequency response of beam tip at different EM parameters (d = 6.5 mm, $A_{ex} = 2g$, $\zeta = 0.024$).

Fig.4 shows the comparison between tip FR curves, at three different damping ratio. Increasing the damping parameter lead to decreast the tip deflection around two resonances, specially at peak responsees. At second peak, the max. of tip deflrction decresed from *A= 081mm* (at *204 Hz*) to *A=0.77 mm* (at *200 Hz*) and *A=0.69 mm* (at *194 Hz*), By doubling and quadrupling of damping, respectively. Also, the internal damping has insignificant effects on excitation bandwith.

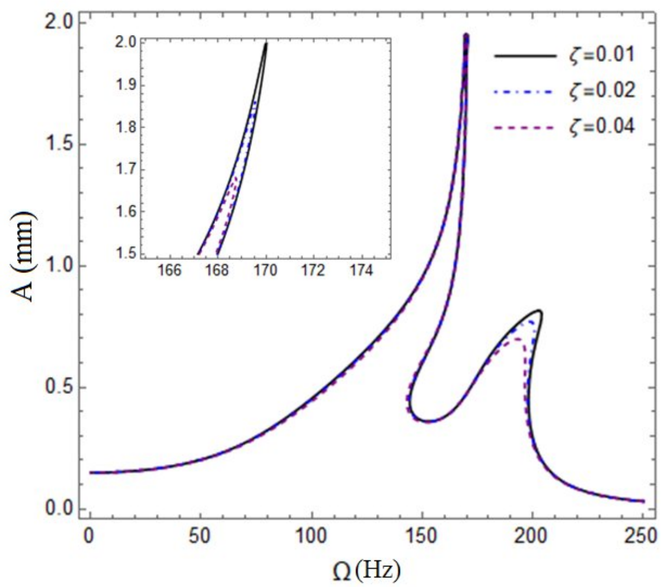

Fig.4
Frequency response versus frequency of the excitation for different damping ratio.

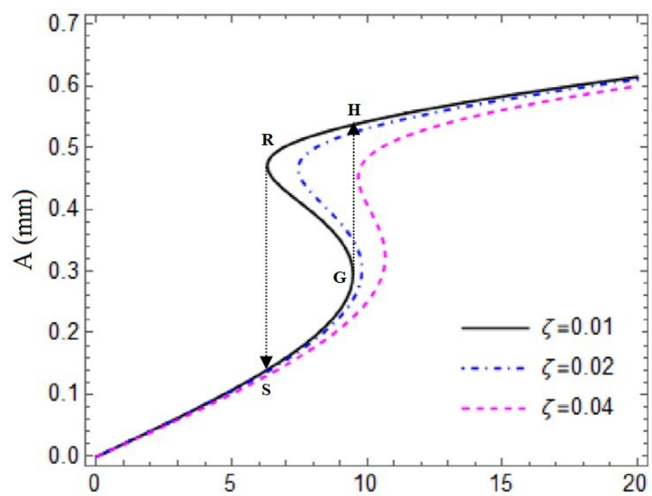

Fig.5
Beam response versus level of the base excitation for different damping ratio (Ω = 120 Hz), with $r_m = r_k = 10$.

The relations between the oscillation amplitude and the excitation level with different damping parameters at $\Omega = 120\ Hz$ are illustrated in the Fig.5 with $r_m = r_k = 10$. The jump phenomena looks at a higher excitation level with increasing damping. this phenomena occurred for $\zeta = 0.01$ at $A_{ex} = 0.94\ g$ and for $\zeta = 0.04$ at $A_{ex} = 1.08\ g$. The plot also demonstrated the higher damping cause lower motion amplitude and narrower unstable region.

Based on the Fig. 5, there are two jump points in each response curve; for instance with $\zeta = 0.01$, the jump occurred at G→H for increasing excitation value, and R→S for decreasing excitation value. When damping parameters increased, two bifurcation points occurs at higher excitation values, also the range of instability for excitation level (A_{ex}) became narrower and system have larger stability range. Based on Fig.5, the instability range (have unstable response and branch) for system with $\zeta = 0.01$ is equal to $6.1\ m/s^2 < A_{ex} < 9.1\ m/s^2$. Moreover for the case $\zeta = 0.02$, the instability range is $7.3\ \text{m/s}^2 < A_{ex} < 9.9\ \text{m/s}^2$ and for the case $\zeta = 0.01$, the instability range is $9.2\ m/s^2 < A_{ex} < 10.4\ m/s^2$.

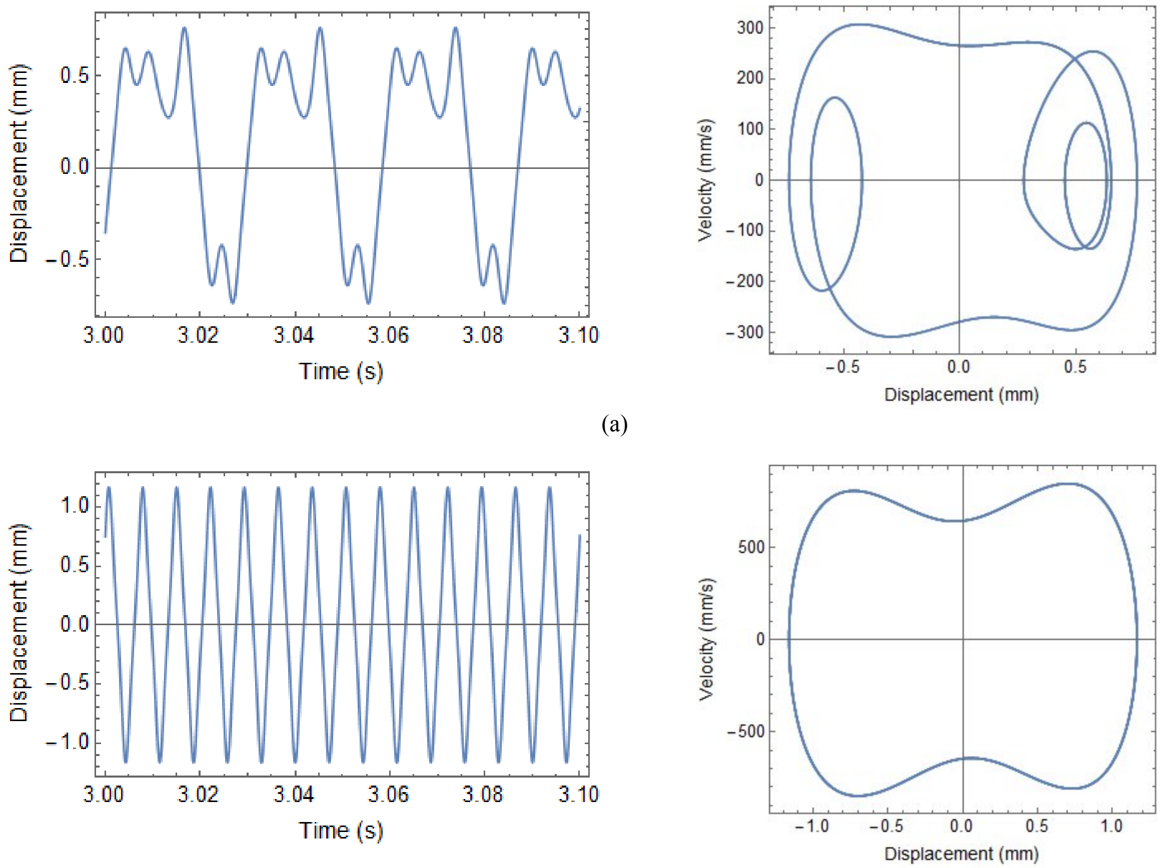

(b)

Fig.6
time response and phase portrait of the tip beam oscillation at different A_{ex} ; (a)1.4g , (b) 2.2g.

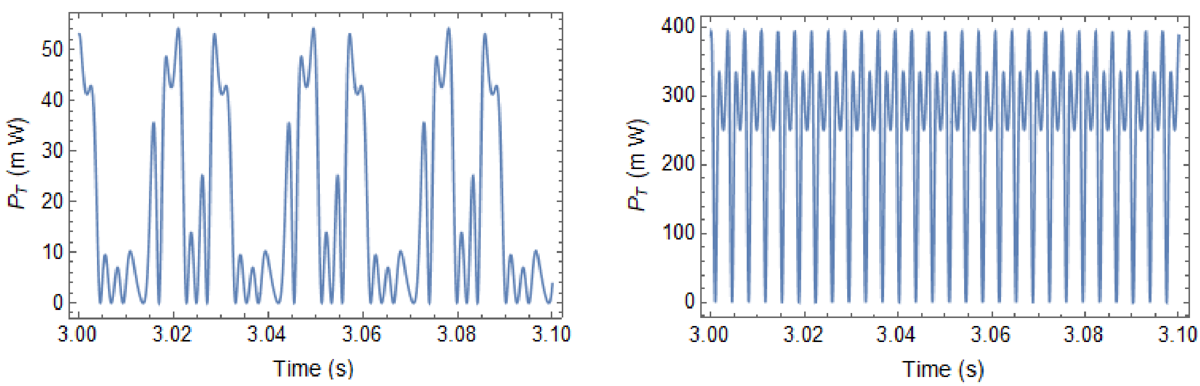

(a) **(b)**

Fig.7
Comparison of the total power of hybrid harvester at two different values of A_{ex} ; (a)1.4g , (b) 2.2g.

The Runge-Kutta method has been used to solve Eq. (20) to study the output features of the hybrid harvester. As shown in Fig.6 vibration amplitude and phase diagram of beam tip are plotted at different excitation levels (base accelaration) when $d = 6.9\ mm$, $r_m = r_k = 5$. With lower A_{ex} , the result shows chaotic motion in Fig. 6(a). Besides based on Fig. 6(b) the beam tip displays a high-energy inter-well motion, considered by a periodic oscillation with high amplitude vibration.

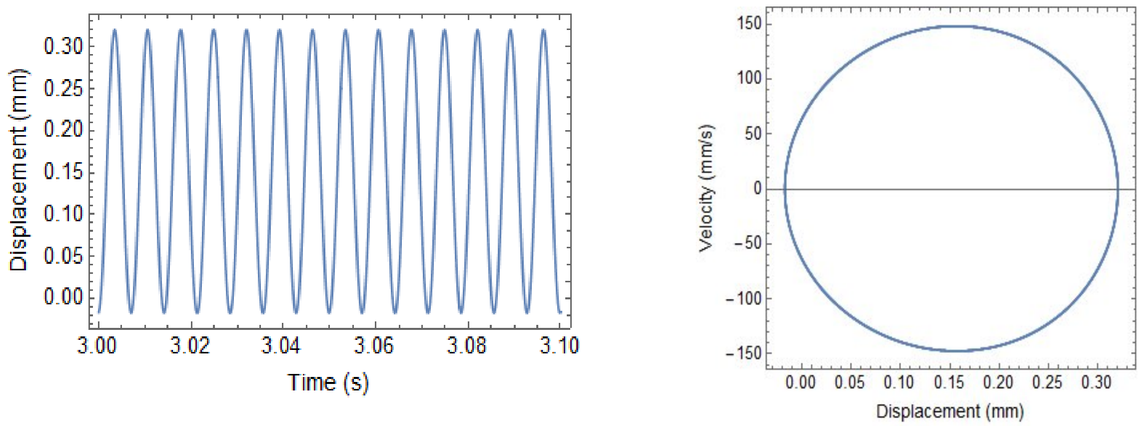

(a)

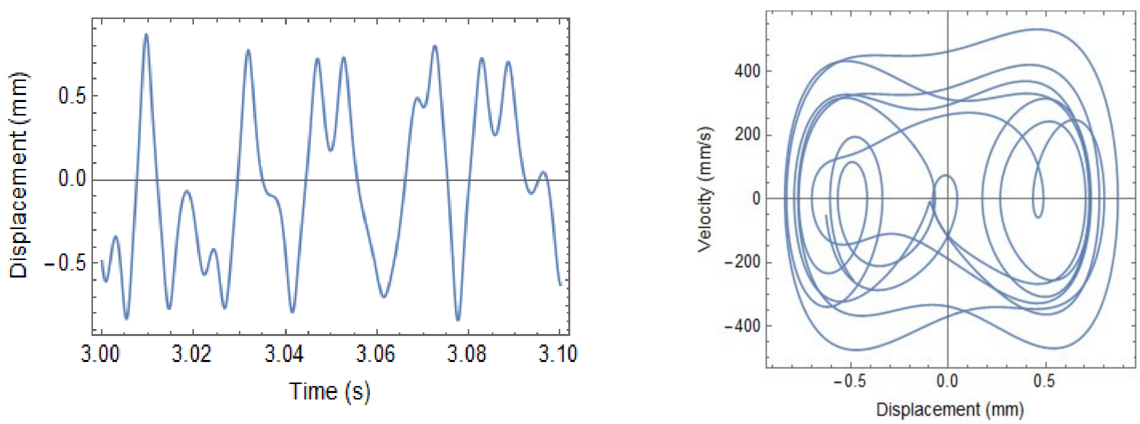

(b)

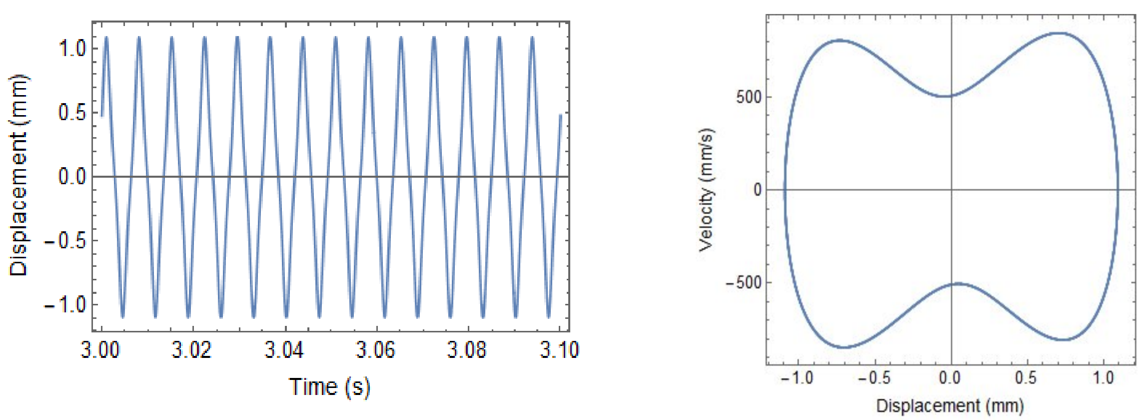

(c)

Fig.8
Time response of the harvested voltage and phase portrait diagram of beam tip at different parameter “d” ; (a)7.4 mm, (b) 6.9 mm, (c) d=6.4 mm.

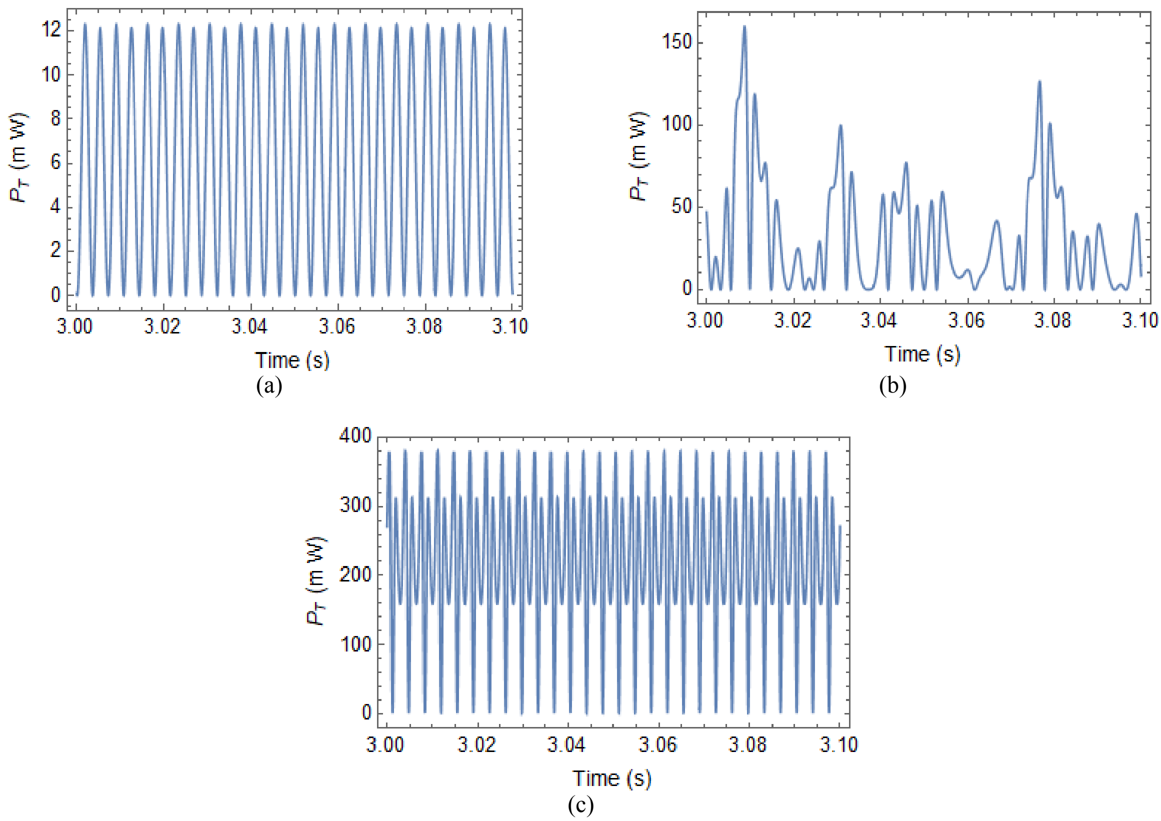

Fig.9
Harvested power versus time for different parameter d ; (a) 7.4 mm, (b) 6.9 mm, (c) d = 6.4mm.

The total generated power of harvester has been plotted at Fig.7 for various A_{ex} amplitudes.

The dynamic response and phase plane diagram of beam tip has been plotted at Fig.8 for various *d* parameter. At fig. 8a , the beam oscillates about an equilibrium point with very small tip velocity and vibrations, cause the intra-well motion and low harvested power. If the distance “d” decreased (fig. 8b) , the output power is chaotic due to tip motion between two wells .By extra decreasing the *“d”* (fig. 8c), the beam tip shows a high-energy inter-well motion, considered by a periodic oscillation with high amplitude, cause the substantial increase of vibration amplitudes and stored power. The total harvested power of harvester has been plotted at Fig.9 for various *“d”* amplitudes.

5 CONCLUSIONS

By investigation of the electromechanical coupled model, this paper attempts to analyze 2DOF hybrid VEH system using the HBM and discusses the effects of base acceleration, excitation frequency, magnets distance and damping on the beam response and output electrical power.The harvesting system includes two vibration DOFs and two electrical DOFs. The employed principle and the corresponding theoretical model of VEH are explained in detail and established based on lumped parameter. The 2DOF model and the frequency response analytical expressions of the hybrid MS-P VEH+EM are obtained, and the properties of harvester are considered. Numerical results showed that:

- By changing the ‘d’ parameter, the beam can show numerous oscillation forms, including intrawell periodic low-energy oscilation (small-amplitude motion), interwell chaotic oscilation and interwell periodic high-energy oscilation (large-amplitude motion).
- The EM could deeply enhance the generating power and broader exciting frequency band.

- Because of the nonlinear repulsive magnetic force, when the cantilever oscillator is in small-amplitude periodic motion or chaotic motion, under a certain distance'd', it can show bistable features in a large frequency band and enter the steady-state situation through the potential well to rise the collected power and the resonance bandwidth.
- The material damping could decrease peak responses, but had insignificant effects on resonance bandwith.
- As shown at frequency response curves, by reducing "d" from 7mm to 5mm, the secound response peak occures at higher frequencies. The peak amplitude were also strongly influenced by this parameter and have been decreased about 10 times.
- By increasing r_m and r_k , the first peak shifted to the right slowly and amplitude of two peaks enlarged.
- When damping parameters increased, two bifurcation points occurs at higher excitation values.

REFERENCES

[1] Beeby S. P. et al., 2007, A micro electromagnetic generator for vibration energy harvesting, *J. Micromechanics microengineering*, 17(7): 1257.

[2] Liu H., Li W., Sun X., Cong C., Cao C., Zhao Q., 2021, Enhanced the capability of magnetostrictive ambient vibration harvester through structural configuration, pre-magnetization condition and elastic magnifier, *J. Sound Vib*., 492: 115805.

[3] Andò B., Baglio S., Bulsara A. R., Marletta V., Pistorio A., 2017, Investigation of a nonlinear energy harvester, *IEEE Trans. Instrum. Meas.*, 66(5): 1067-1075.

[4] Tang L., Yang Y., Soh C. K., 2012, Improving functionality of vibration energy harvesters using magnets, *J. Intell. Mater. Syst. Struct.*, 23(13): 1433-1449.

[5] Ferrari M., Ferrari V., Guizzetti M., Andò B., Baglio S., Trigona C., 2010, Improved energy harvesting from wideband vibrations by nonlinear piezoelectric converters, *Sensors Actuators A Phys.*, 162(2): 425-431.

[6] Karami M. A., Inman D. J., 2011, Equivalent damping and frequency change for linear and nonlinear hybrid vibrational energy harvesting systems, *J. Sound Vib*., 330(23): 5583-5597.

[7] Kim P., Seok J., 2014, A multi-stable energy harvester: Dynamic modeling and bifurcation analysis, *J. Sound Vib*., 333(21): 5525–5547.

[8] Jiang J., Liu S., Zhao D., Feng L., 2019, Broadband power generation of piezoelectric vibration energy harvester with magnetic coupling, *J. Intell. Mater. Syst. Struct*., 30(15): 2272-2282.

[9] Nguyen M. S., Yoon Y. J., Kim P., 2019, Enhanced broadband performance of magnetically coupled 2-DOF bistable energy harvester with secondary intrawell resonances, *Int. J. Precis. Eng. Manuf. Technol*., 6(3): 521-530.

[10] Wang L., Chen R., Ren L., Xia H., Zhang Y., 2019, Design and experimental study of a bistable magnetoelectric vibration energy harvester with nonlinear magnetic force scavenging structure, *Int. J. Appl. Electromagn. Mech*., 60(4): 489-502.

[11] Kianpoor A., Jahani K., 2019, Modeling and analyzing of energy harvesting from trapezoidal piezoelectric beams, *Iran. J. Sci. Technol. Trans. Mech. Eng.*, 43(1): 259-266.

[12] Heshmati M., Amini Y., 2020, An electromechanical finite element model for new CNTs-reinforced harvesters subjected to harmonic and random base excitations, *Iran. J. Sci. Technol. Trans. Mech. Eng*., 44(1): 163-181.

[13] Rezaei M., Talebitooti R., Friswell M. I., 2019, Efficient acoustic energy harvesting by deploying magnetic restoring force, *Smart Materials and Structures*, 28(10): 105037.

[14] Rezaei M., Talebitooti R., 2022, Investigating the performance of tri-stable magneto-piezoelastic absorber in simultaneous energy harvesting and vibration isolation, *Applied Mathematical Modelling*, 102: 661-693.

[15] Rezaei M., Talebitooti R., Rahmanian S., 2019, Efficient energy harvesting from nonlinear vibrations of PZT beam under simultaneous resonances, *Energy*, 182: 369-380.

[16] Aladwani A., Arafa M., Aldraihem O., Baz A., 2012, Cantilevered piezoelectric energy harvester with a dynamic magnifier, *J. Vib. Acoust*., 134,(3): 31004.

[17] Vasic D., Costa F., 2013, Modeling of piezoelectric energy harvester with multi-mode dynamic magnifier with matrix representation, *Int. J. Appl. Electromagn. Mech*., 43(3): 237-255.

[18] Wang G. Q., Liao W. H., 2016, A bistable piezoelectric oscillator with an elastic magnifier for energy harvesting enhancement, *J. Intell. Mater. Syst. Struct.*, 28(3): 392-407.

[19] Wang G., Liao W. H., Yang B., Wang X., Xu W., Li X., 2018, Dynamic and energetic characteristics of a bistable piezoelectric vibration energy harvester with an elastic magnifier, *Mech. Syst. Signal Process.,* 105: 427-446.

[20] Bernard B. P. Mann B. P., 2018, Increasing viability of nonlinear energy harvesters by adding an excited dynamic magnifier, *J. Intell. Mater. Syst. Struct.*, 29(6): 1196-1205.

[21] Liu H., Cong C., Cao C., Zhao Q., 2020, Analysis of the key factors affecting the capability and optimization for

magnetostrictive iron-gallium alloy ambient vibration harvesters, *Sensors*, 20(2): 401.
[22] Ueno T., Yamada S., 2011, Performance of energy harvester using iron--gallium alloy in free vibration, *IEEE Trans. Magn*., 47(10): 2407-2409.
[23] Kita S., Ueno T., Yamada S., 2015, Improvement of force factor of magnetostrictive vibration power generator for high efficiency, *J. Appl. Phys*., 117(17): 17B508.
[24] Fang Z. W., Zhang Y. W., Li X., Ding H., Chen L. Q., 2018, Complexification-averaging analysis on a giant magnetostrictive harvester integrated with a nonlinear energy sink, *J. Vib. Acoust*., 140(2).
[25] Ahmed U., Jeronen J., Zucca M., Palumbo S., Rasilo P., 2019, Finite element analysis of magnetostrictive energy harvesting concept device utilizing thermodynamic magneto-mechanical model, *J. Magn. Magn. Mater*., 486: 165275.
[26] Cao S., Liu L., Zheng J., Pan R., Song G., 2019, Modeling and Analysis of Galfenol Nonlinear Cantilever Energy Harvester with Elastic Magnifier, *IEEE Trans. Magn*., 55(6): 1-5.
[27] Zhang Y. W., Gao C. Q., Zhang Z., Zang J., 2021, Dynamic analysis of vibration reduction and energy harvesting using a composite cantilever beam with Galfenol and a nonlinear energy sink, *Int. J. Appl. Mech*., 13(08): 2150089.
[28] Liu H., Zhao L., Chang Y., Cong C., 2021, Design and characteristic analysis of magnetostrictive bistable vibration harvester with displacement amplification mechanism, *Energy Convers. Manag*., 243: 114361.
[29] Goudarzi M., Niazi K., Besharati M. K., 2013, Hybrid energy harvesting from vibration and temperature gradient by PZT and PMN-0.25 PT ceramics, *Mater. Phys. Mech.*, 16(1): 55.
[30] Wang H., Tang L., Guo Y., Shan X., Xie T., 2014, A 2DOF hybrid energy harvester based on combined piezoelectric and electromagnetic conversion mechanisms, *J. Zhejiang Univ*., 15,(9): 711-722.
[31] Sengha G. G., Kenfack W. F., Siewe M. S., Tabi C. B., Kofané T. C., 2020, Dynamics of a non-smooth type hybrid energy harvester with nonlinear magnetic coupling, *Commun. Nonlinear Sci. Numer. Simul*., 90: 105364.
[32] Jahanshahi H., Chen D., Chu Y. M., Gómez-Aguilar J. F., Aly A. A., 2021, Enhancement of the performance of nonlinear vibration energy harvesters by exploiting secondary resonances in multi-frequency excitations, *Eur. Phys. J. Plus*, 136(3): 1-22.
[33] Fang S., Xing J., Chen K., Fu X., Zhou S., Liao W. H., 2021, Hybridizing piezoelectric and electromagnetic mechanisms with dynamic bistability for enhancing low-frequency rotational energy harvesting, *Appl. Phys. Lett*., 119(24): 243903.
[34] Li X., Li Z., Liu B., Zhang J., Zhu W., 2022, Numerical research on a vortex shedding induced piezoelectric-electromagnetic energy harvester, *J. Intell. Mater. Syst. Struct*., 33(1): 105-120.
[35] Mihankhah A., Khoddami Maraghi Z., Ghorbanpour Arani A., Niknejad S., 2022, Magneto-Rheological Response in Vibration of Intelligent Sandwich Plate with Velocity Feedback Control, *Journal of Solid Mechanics*, 14,(4): 430-446.
[36] Miraliyari O., Jafari Mehradadi S., Najafizadeh M. M., 2023, Nonlinear Free Vibration Analysis of Functionally Graded Sandwich Beam with Magnetorheological Fluid Core Using Timoshenko Beam Theory, *Journal of Solid Mechanics*, 15(2): 120-143.
[37] Niazi K., Kazemzadeh-Parsi M. J., Mohammadi M., 2022, Nonlinear Dynamic Analysis of Hybrid Piezoelectric-Magnetostrictive Energy-Harvesting Systems, *Journal of Sensors*, doi:10.1155/2022/8921779.
[38] Erturk A., Inman D. J., 2008, On mechanical modeling of cantilevered piezoelectric vibration energy harvesters, *J. Intell. Mater. Syst. Struct.*, 19(11): 1311-1325.
[39] Cao S., et al., 2018, Modeling and analysis of Galfenol cantilever vibration energy harvester with nonlinear magnetic force, *AIP Adv.*, 8(5): 56718.
[40] Cao S., et al., 2015, Dynamic characteristics of Galfenol cantilever energy harvester, *IEEE Trans. Magn*., 51(3): 1-4.
[41] Paswan B., Singh P., Sanjeev A. Sahu, 2023, Mathematical Study for the Rayleigh Wave Propagation in a Composite Structure with Piezoelectric Material, *Journal of Solid Mechanics*, 15(2): 144-159.
[42] Sobamowo M.G., 2022, Analysis of Nonlinear Vibration of Piezoelectric Nanobeam Embedded in Multiple Layers Elastic Media in a ThermoMagnetic Environment Using Iteration Perturbation Method, *Journal of Solid Mechanics*, 14(2): 221-251.
[43] Shu S., 2012, Dynamic modeling and analysis of a bistable piezoelectric cantilever power generation system, *Acta Phys. Sin*, 61(21): 1-12.
[44] Karkar S., Cochelin B., and Vergez C., 2014, A comparative study of the harmonic balance method and the orthogonal collocation method on stiff nonlinear systems, *J. Sound Vib*., 333(12): pp. 2554–2567.